Chapter 2 Theory of Optical Phase lock Loops

A Phase Lock Loop (PLL) is a negative feedback control system, which forces a local oscillator (LO) to track the frequency and phase of a reference signal within the loop bandwidth. This same idea can be used to construct an Optical Phase Lock Loop (OPLL), in which a slave laser tracks the frequency and phase of the optical signal of a master laser. In this chapter, I will study the theory of an OPLL in detail. I will first summarize the basic concept and theory of OPLLs and present both the time domain and the frequency domain analyses of an OPLL. I will then linearize the system using the small signal approximation and utilize the transfer function methodology to study the stability, acquisition range, holding range, and the residual phase noise of the OPLLs. Finally the effect of the loop delay and the non-uniform FM response will be considered.

2.1 Principle of operation

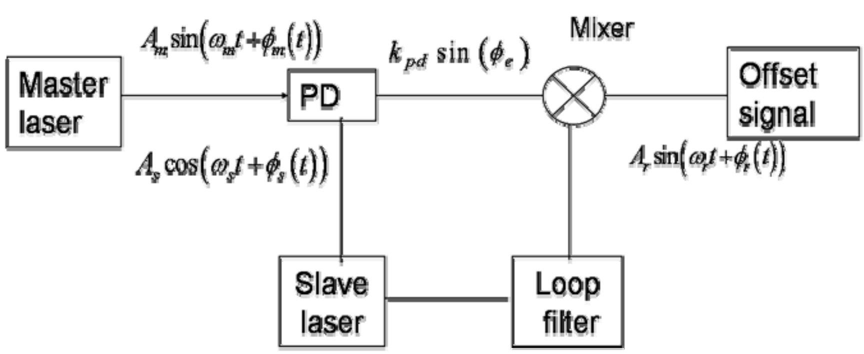

Fig. 2.1 Schematic diagram of an OPLL.

A schematic diagram of a typical heterodyne OPLL is plotted in Fig. 2.1. The optical signals of the master laser $A_m \sin(\omega_m t + \phi_m)$ and the slave laser $A_s \sin(\omega_s t + \phi_s)$ are combined at a photodetector, which detects the phase and frequency differences. The output of the photodetector is further mixed with a reference signal $A_r \sin(\omega_r t + \phi_r)$. The down-converted phase error signal passes through a loop filter and is fed back to the slave laser. The frequency and phase of the slave laser are modulated by the feedback current, and are forced to track those of the master laser with a frequency and phase offset determined by the reference signal. A rigorous analysis of the OPLLs can be performed in either the time domain or the frequency domain.

2.2 Time domain analysis

The operation principle of an OPLL is very similar to the well-studied electronic PLLs. Therefore the theoretical analysis of OPLL can be directly borrowed from the theoretical framework of PLLs[1, 2]. In Fig. 2.1 the photodetector and the radio frequency (RF) mixer together play the role of a phase detector. The master laser signal and the slave laser signal are mixed and fed into the photodetector (with a built-in trans-impedance amplifier), the resulting output is given by

$$v_1(t) = 2R_{pd}\sqrt{P_m P_s}\sin\left[\left(\omega_m - \omega_s\right)t + \phi_m(t) - \phi_s(t)\right] \tag{2.1}$$

where R_{pd} is the responsivity of the photodetector, P_m and P_s are the optical power of the master laser and the slave laser respectively. $v_1(t)$ is further mixed with a RF reference signal $E_r = A_r\cos\left(\omega_r t + \phi_r(t)\right)$ using a RF mixer. Neglecting the sum frequency term, the down-converted phase error current signal provided by the mixer is

$$i(t) = K_{pd}\sin\phi_e = K_{pd}\sin\left[\left(\omega_m - \omega_s - \omega_r\right)t + \phi_m(t) - \phi_s(t) - \phi_r(t)\right] \tag{2.2}$$

where $K_{pd} = \eta R_{pd}\sqrt{P_m P_s}A_r$ is defined as the gain of the phase detector, and η is the current responsivity of the RF mixer. Care must be taken when determining η since most mixers are neither ideal current sources nor ideal voltage sources, and η also depends on the load applied to the output port of the mixer. The down-converted phase error signal is fed back to the slave laser, whose phase is modulated as

$$\frac{d\phi_s(t)}{dt} = K_s \cdot \{ i(t) * f_{flt}(t) * f_s(t) \} \tag{2.3}$$

where K_s is the current FM sensitivity of the slave laser and $f_{flt}(t)$ and $f_s(t)$ are the impulse response of the loop filter and the slave laser respectively. By setting all the d/dt terms equal to zero in Eq. (2.3), the steady state solution is obtained as

$$\begin{aligned} &\omega_s = \omega_m - \omega_r \ , \ \ \phi_s = \phi_m - \phi_r - \phi_{e0} \\ &sin(\phi_{e0}) = (\omega_m - \omega_{s,fr} - \omega_r) / K_{dc} \end{aligned} \tag{2.4}$$

where $\omega_{s,fr}$ is the frequency of the free-running slave laser, $K_{dc} = K_{pd} K_f K_s$ is the loop DC gain, K_f is the DC response of the loop filter, and ϕ_{e0} is the steady state phase error. Eq. (2.4) shows that the frequency and phase difference between the locked slave laser and the master laser are set by the RF reference signal. This configuration is called heterodyne OPLL. If there is no frequency offset, i.e., $\omega_r = 0$, when the loop is in lock $\omega_s = \omega_m$ and the system becomes a homodyne OPLL. The analyses of heterodyne and homodyne OPLLs are similar, except that the frequency and phase of the RF reference signal have to be considered in Eq. (2.2) and the conversion gain of the mixer has to be included while calculating the loop gain. For the sake of simplicity, I will use the homodyne OPLL scheme to perform the analysis in the remainder of the thesis, unless explicitly stated otherwise.

In general Eq. (2.3) is a complex nonlinear differential equation involving convolutions and there is no simple analytic solution. To understand the fundamental dynamic process of this feedback control system, I assume that the response of the slave laser is instantaneous, i.e., $f_s(t) = \delta(t)$. Ignoring the loop filter and using the dynamic variable $\phi_e = \phi_m - \phi_s$, Eq. (2.3) reduces to

$$\phi_e'(t) + K_{dc} \sin\phi_e(t) = \phi_m'(t) \tag{2.5}$$

where $K_{dc} = K_{pd} K_s$ is the loop DC gain. Assuming a small phase error $\phi_e(t) << 1$, the solution to this differential equation takes the form

$$\phi_e(t) = e^{-K_{dc}t} \int e^{-K_{dc}t'} \phi_m'(t')dt' + ce^{-K_{dc}t} \quad (2.6)$$

It is instructive to look at two simple cases. The first case is one starting with a constant phase error, i.e., $\phi_e(0) = \Delta\phi$, then the solution is

$$\phi_e(t) = \Delta\phi e^{-K_{dc}t} \quad (2.7)$$

Eq. (2.7) corresponds to an exponentially decaying phase error with a time constant $1/K_{dc}$, so that the phase of the slave laser eventually tracks the phase of the master laser. The loop gain K_{dc} determines the speed of phase-tracking, or the loop bandwidth.

Another typical case is one of a phase ramp $\phi_m(t) = \Delta\omega \cdot t$. This is the case when there exists an initial frequency offset $\Delta\omega$ between the slave laser and the master laser. The solution to this case is

$$\phi_e(t) = \frac{\Delta\omega}{K_{dc}}\left(1 - e^{-K_{dc}t}\right) \quad (2.8)$$

In this case in the limit $t \to \infty$ there is a nonzero steady state phase error

$$\phi_{e0} = \Delta\omega / K_{dc} \quad (2.9)$$

which results in a constant feedback current, that forces the frequency of the slave laser to track that of the master laser. Eqs. (2.7) and (2.8) show that the function of an OPLL is to force the phase and frequency of the slave laser to track that of the master laser.

2.3 Frequency domain analysis

2.3.1 Transfer function method

Frequency domain analysis is a more convenient and powerful tool in characterizing OPLLs. In the time domain, solving Eq. (2.3) involves a complicated and time-consuming convolution algorithm. In the frequency domain, Eq. (2.3) involves only products of Fourier transforms, i.e., the transfer functions. The performance of OPLLs such as their stability, the loop bandwidth, the compensation filter design can be analyzed by means of the transfer function formalism and Bode plots.

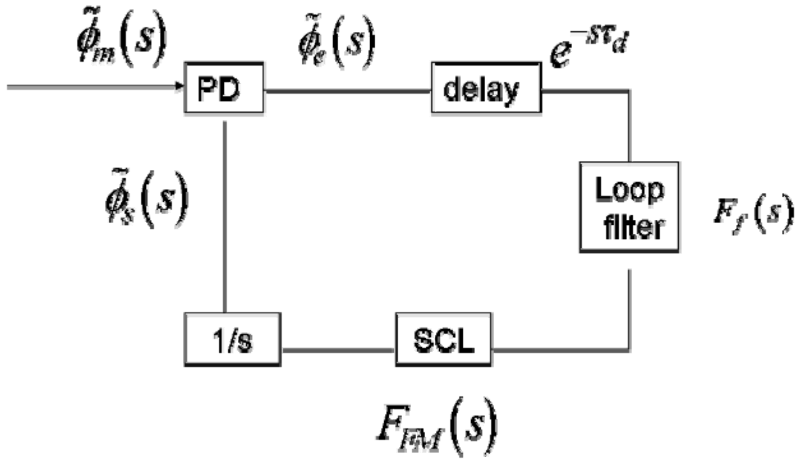

Fig. 2.2 The frequency domain representation of OPLLs.

The schematic frequency domain representation of a homodyne OPLL is shown in Fig. 2.2. $s = j\omega$ is the Laplace variable, $\exp(-s\tau_d)$ represents the delay of the loop, $F_f(s)$ is the normalized transfer function of the loop filter, and $F_{FM}(s)$ is the normalized transfer function of the FM response of the slave laser. The 1/s block originates from the fact that the phase ϕ, which is the dynamic variable, is the integration of the frequency over time. By using the small signal perturbation to linearize Eq. (2.3) about the steady state locking point ϕ_{e0}, and taking the Fourier transform, the open loop transfer function is derived as

$$G_{op}(s) \equiv \frac{\phi_s(s)}{\phi_e(s)} = \frac{K'_{dc} F_f(s) F_{FM}(s) \exp(-s\tau_d)}{s} \tag{2.10}$$

where $K'_{dc} = K_{dc} \cos\phi_{e0}$. The closed loop signal transfer function is defined as

$$H_o(s) \equiv \frac{\phi_s(s)}{\phi_m(s)} = \frac{G_{op}(s)}{1+G_{op}(s)} = \frac{K'_{dc}F_{FM}(s)F(s)\exp(-s\tau_d)}{s+K'_{dc}F_{FM}(s)F(s)\exp(-s\tau_d)} \tag{2.11}$$

and the error transfer function is

$$H_e(s) \equiv \frac{\phi_e(s)}{\phi_m(s)} = \frac{1}{1+G_{op}(s)} = 1-H_o \tag{2.12}$$

The closed loop signal transfer function $H_o(s)$ acts as a low pass filter, which means that the phase of the slave laser tracks the phase of the master laser within the bandwidth of the filter. On the other hand, the phase error transfer function $H_e(s)$ behaves as a high pass filter. The differential phase error within the loop bandwidth is thus suppressed by the OPLL. In practice, the loop bandwidth is limited mainly by the non-negligible loop delay and the non-uniform FM response of the slave laser. These issues will be discussed in detail in Section 2.5.

2.3.2 Acquisition and holding range

Two important parameters describing the locking capability and the stability of the OPLL are the acquisition range Δf_{acq} (the maximal frequency difference between the free-running slave laser and the master laser for the OPLL to acquire lock), and the holding range Δf_h (the maximal frequency difference between the free-running slave laser and the master laser for the OPLL to stay in lock). The acquisition and holding ranges of a PLL generally depend on the loop gain and the loop order[32].

First order PLL

The first order PLL is defined as one with no loop filter, i.e., $F_f(s)=1$. If I assume that the slave laser has a flat frequency modulation response $F_{FM}(s)=1$, then the open loop gain is found from Eq. (2.10) as

$$G(s) = \frac{K_{dc}}{s}e^{-s\tau_d} \tag{2.13}$$

In this case, the acquisition and holding ranges are simply[1]

$$\Delta f_{acq} = \Delta f_h = K_{dc} / 2\pi \tag{2.14}$$

Second-order PLL

Traditionally three types of loop filters are typically used to make the second-order PLL: the lowpass(LP) filter, the passive lead-lag (or lag-lead) filter, and the active second-order filter. An active second-order filter has a transfer function of

$$F(s) = \frac{1+\tau_2 s}{\tau_1 s} \tag{2.15}$$

Since this type of filter has an integration term $1/s$, the loop has very high open loop gain at low frequency and provides the best performance with respect to phase noise reduction[1]. The acquisition and holding ranges are theoretically infinite for such a loop filter.

2.3.3 Bode plot and stability criterion

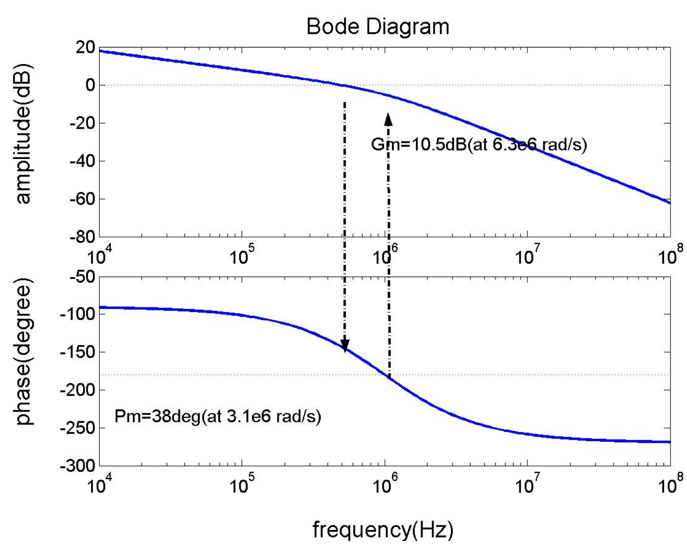

Fig. 2.3 The Bode plot of a PLL with a second-order low pass filter. The gain margin is $G_m = 10.5\ dB$ and the phase margin is $P_m = 38^0$.

The Bode plot is a powerful graphic tool in studying the performance and stability of

PLLs especially when various compensation filters are included. Fig. 2.3 shows the Bode plot of a PLL with a second-order low pass loop filter, in which both the amplitude $\left|G_{op}\left(j\omega\right)\right|$ (dB scale) and the phase $Arg\left[G_{op}\left(j\omega\right)\right]$ (in degrees) are plotted as a function of the frequency.

Stability criterion: The stability criterion of an OPLL can easily be derived from its Bode plot: if the amplitude of $G_{op}\left(s\right)$ crosses 0 dB at only one frequency, the amplitude $\left|G\left(j\omega_{\pi}\right)\right|$ must be smaller than 1 at the π phase lag frequency ω_{π} ($\angle G_{op}\left(j\omega_{\pi}\right)=-180^{o}$). Equivalently, the phase lag $\angle G_{op}\left(j\omega_{gc}\right)$ must be bigger than -180^{o} at the gain crossover frequency ω_{gc} ($\left|G_{op}\left(j\omega_{gc}\right)\right|=1$)[1]. This can be understood by the following intuitive reasoning. At the π phase lag frequency ω_{π} the original negative feedback system becomes a positive feedback system. If the amplitude of the loop gain is higher than 1, any noise in the system will be amplified in each round-trip, eventually leading to oscillations.

Stability margins

Based on the stability criterion, one can define two stability margins: the phase margin is defined as $\angle G_{op}\left(j\omega_{gc}\right)+\pi$, and the gain margin is defined as $-20\log\left|G_{op}\left(j\omega_{\pi}\right)\right|dB$. Sufficient phase margin or gain margin are necessary to guarantee the stability of the loop. Based on the time domain simulation, the gain margin is generally chosen to be within the range 8~10 dB to suppress excessive ringing during the acquisition[33].

2.4 Loop noise characterization

In an OPLL, various noise sources affect the loop performance and need to be considered. Among these noise sources, the phase noise of the SCLs, is the dominant one, since SCLs typically possess a linewidth between hundreds of KHz and a few MHz. Other noise sources include the photodetector shot noise and the electronics noise. A schematic diagram of the various phase noise sources and their points of entry in an OPLL is shown in Fig. 2.4. The phase noise of the master laser and the slave laser are accounted for by ϕ_m^n and ϕ_s^n. ϕ_{sn} stands for the photodetector shot noise. The electronics noise is small and can be ignored.

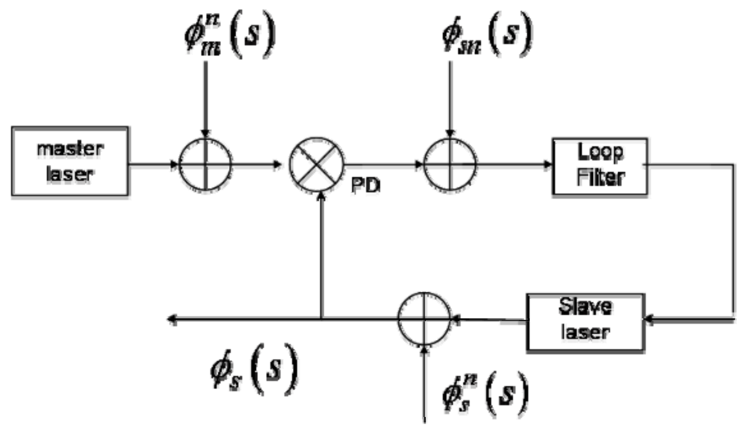

Fig. 2.4 Sources of phase noise in an OPLL

Following the standard negative feedback analysis, one obtain the phase of the locked slave laser and the differential phase error as

$$\phi_s(s) = \left(\phi_m + \phi_m^n\right) \cdot H_o + \phi_{sn} / K_{pd} \cdot H_o + \phi_s^n \cdot H_e \tag{2.16}$$

$$\phi_e(s) = \left(\phi_m + \phi_m^n + \phi_s^n\right) \cdot H_e + \phi_{sn} / K_{pd} \cdot H_o \tag{2.17}$$

The corresponding spectral power density functions are

$$S_s(f) = \left[S_m(f) + S_{sn}(f) / K_{pd}^2\right] \left|H_o(f)\right|^2 + S_{s,fr}(f) \left|H_e(f)\right|^2 \tag{2.18}$$

$$S_e(f) = \left[S_m(f) + S_{s,fr}(f)\right] \cdot \left|H_e(f)\right|^2 + S_{sn}(f) / K_{pd}^2 \cdot \left|H_o(f)\right|^2 \tag{2.19}$$

where $S_{s,fr}, S_m, S_{sn}$ are, respectively, the spectral density functions of phase noise of the free-running slave laser, the phase noise of the master laser, and the shot noise.

Here I will only use the differential phase error to characterize the noise level of an OPLL. A detailed analysis and measurement of the phase noise of the slave laser in an OPLL will be given in Chapter 6 (Coherence cloning using OPLLs). Assuming that the frequency noise of the lasers has a white Gaussian distribution, the double-sided spectral densities of the different noise sources are given by [19]

$$S_m(f)=\frac{\Delta f_m}{2\pi f^2},\ \ S_s(f)=\frac{\Delta f_s}{2\pi f^2},\ S_{sn}(f)=2eR\left(P_s+P_m\right) \tag{2.20}$$

where Δf_m and Δf_s are the FWHM linewidths of the master laser and the free-running slave laser, R is the responsivity of the photodetector. Fig. 2.5 shows the power spectral density of the differential phase error ϕ_e in a typical OPLL with a loop delay of 100 ns. At low frequencies, the phase error is significantly reduced by the feedback loop. As the loop gain increases, the bandwidth and ratio of the noise reduction increase. However, as the gain approaches the maximum allowable loop gain, as per the stability criterion, a spectral peak appears and the noise at the corresponding frequency is significantly amplified. In Fig. 2.5(b) an active second-order filter $\left(1+f/f_0\right)/\left(f/f_0\right)$ is used to further reduce the phase noise at low frequencies.

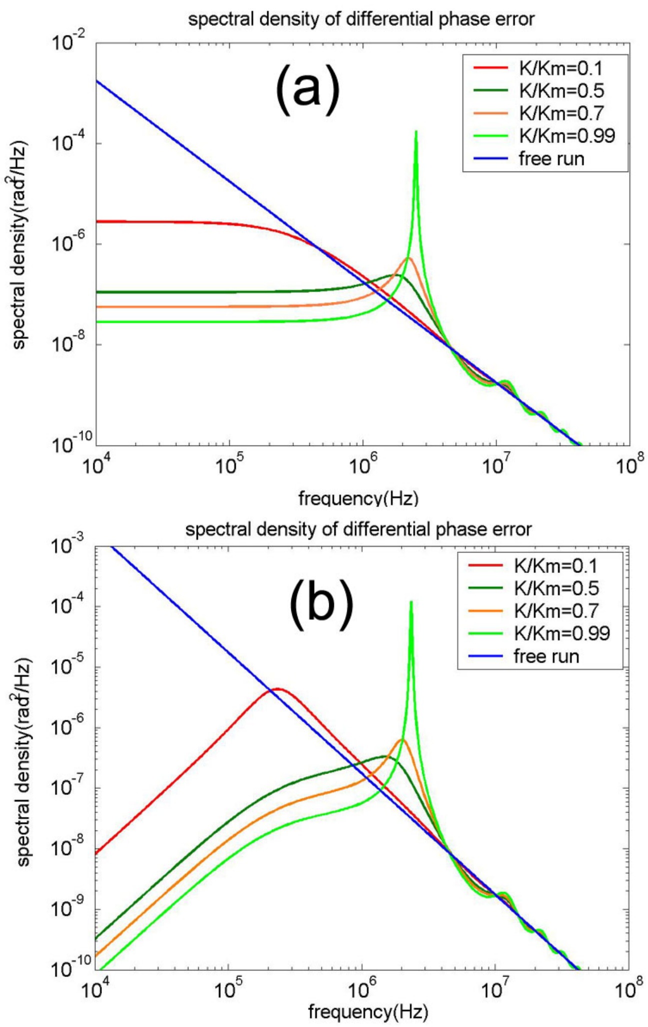

Fig. 2.5 The spectral density functions of the differential phase error ϕ_e for different small signal loop gain *K*. K_m is the maximum allowable loop gain determined by the stability criterion. (a) No loop filter is used. (b) An active second-order filter $\left(1+f/f_0\right)/\left(f/f_0\right)$ is used. In both (a) and (b), a loop delay of 100 ns is assumed.

An important parameter called the phase error variance can be obtained by integrating the phase noise spectral density over all frequencies

$$\sigma^2 = \int_{-\infty}^{\infty} S\left(f\right)df \tag{2.21}$$

Thus the variance of the differential phase error is

$$\sigma_{\phi_e}^2 = \int_{-\infty}^{+\infty} S_{\phi_e} df = \int_{-\infty}^{+\infty} \left[S_m(f) + S_{s,fr}(f) \right] \cdot \left| H_e(f) \right|^2 + S_{sn}(f) / K_{pd}^2 \cdot \left| H_o(f) \right|^2 df \quad (2.22)$$

Combining Eq. (2.20) with the definitions

$$B_n = \int_0^\infty H_o(f) df \text{ and } I_p = \int_0^\infty H_e(f) / f^2 df \quad (2.23)$$

Eq. (2.22) is simplified to

$$\sigma_{\phi_e}^2 = \frac{\Delta f}{\pi} I_p + \frac{eB_n (P_m + P_s)}{RP_m P_s} \quad (2.24)$$

where $\Delta f = \Delta f_m + \Delta f_s$ is the sum of the linewidths of the master laser and the slave laser.

In the presence of phase noise, the loop loses lock through cycle slipping (the output phase error rotates through 2π after initially starting at zero)[1], and the noise in the OPLL can be evaluated by the average time between cycle slips T_{cs}. For the first order, the modified first-order, and the second-order type II loops, T_{cs} is related to σ^2 by, respectively[1]

$$T_{cs-I} \simeq \pi e^{2/\sigma^2} / 4B_n, \quad T_{cs-II} \simeq e^{\pi/2\sigma^2} / B_n \quad (2.25)$$

2.5 Practical limitations of the loop bandwidth

In the previous analysis, the bandwidth, acquisition range, holding range and noise reduction capability of an OPLL all rely on one critical parameter: i.e., the loop gain K_{dc}. Therefore, a large, loop gain is desired. However, K_{dc} is limited by two major practical constraints – namely, the non-negligible loop delay and the non-uniform frequency modulation response of SCLs. In this section I will analyze the loop performance limited by these two factors.

2.5.1 The non-negligible loop delay

Loop delay exists in all practical feedback control systems. In the presence of the loop delay, the phase lag increases unbounded as the frequency increases. As described in Section 2.3.3, the stability criterion requires the loop gain to be restricted to less than 1 at the 180 degree phase lag frequency. Hence the loop gain and the resulting loop bandwidth will be limited. In electronic PLLs made of integrated circuits, the length of the loop is at most a few mm and the delay is not a serous concern. In constructing an OPLL, either using micro-optics or using fiber optical components, the delay can be as big as a few ns. As the desired loop bandwidth is equal or greater than tens of MHz, due to the large linewidth of SCLs, the effect of the loop delay at these frequency ranges can't be ignored. Here I first restrict the analysis to the case where the loop bandwidth is only limited by the loop delay. The FM responses of the slave laser and all the electronics are assumed to be ideal. With the above assumption, and in the absence of a loop filter, the open loop transfer function (Eq. (2.10)) is simplified to

$$G_{op}(s) = K'_{dc}\frac{\exp(-s\tau_d)}{s} \tag{2.26}$$

and the 180^0 phase lag frequency is

$$\omega_\pi = \pi/2\tau_d \quad \text{or} \quad f_\pi = 1/4\tau_d \tag{2.27}$$

Considering the stability criterion described in Section 2.3.3, the maximum loop gain K_{dc} is $\pi/2\tau_d$. The resulting maximum holding range and acquisition range are $f_\pi = 1/4\tau_d$. In practice, this number is even smaller since a gain margin of 8~10 dB is needed to avoid excessive ringing.

I have studied the dynamic locking process in the time domain using the Simulink toolbox in MATLAB®. The FM response of the slave laser is assumed to be uniform, and the laser is modeled as an ideal integrator 1/s. As an example, I assume that the delay time is t_d = 5 ns, the frequency difference between the free-running slave laser and the master laser is $\Delta\omega = 2$ MHz. No loop filter is used. The corresponding maximum loop gain in this case is $10\pi \times 10^7\, rad/s$. The simulated temporal dependence of $\sin\phi_e(t)$ is plotted in Fig. 2.6. When the loop gain is $4\pi \times 10^7\, rad/s$ (corresponding to a gain margin of 8dB), the photodetector output $\sin\phi_e(t)$ quickly settles down to the steady state locking point. As the loop gain is increased to $8\pi \times 10^7\, rad/s$, $\sin\phi_e(t)$ converges to the steady state locking point with significant ringing. As the loop gain is further increased to $10.2\pi \times 10^7\, rad/s$, the loop becomes unstable and starts oscillating. From this time domain simulation, one can see that a gain margin of at least 8 dB is needed to suppress ringing effects.

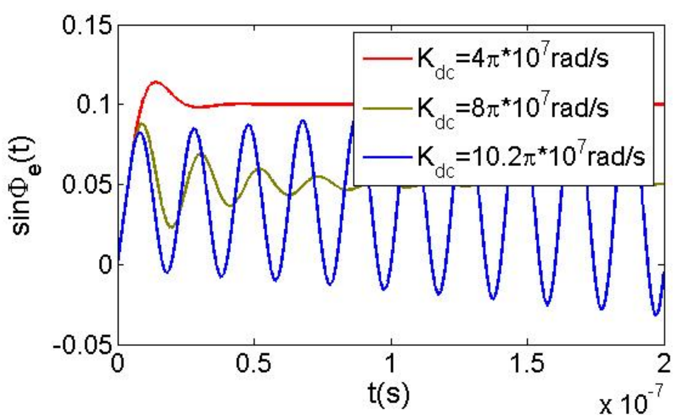

Fig. 2.6 Temporal dependence of $\sin\phi_e$ for different DC loop gain K_{dc}. A loop delay of 5 ns and a free-running frequency difference of 2 MHz are assumed in the simulation.

The variance of the differential phase error can be calculated according to Eq. (2.22). Using the parameters $P_m = P_s = 1mW$, R = 0.5A/W, and a gain margin of 8 dB, I calculate the variance of the differential phase error as a function of the loop delay and the summed linewidth of the lasers. From the calculation one observes that the variance of the differential phase error is only dependent on the summed linewidth normalized by the π phase lag frequency, i.e. $\Delta f / f_\pi$, not on the absolute value of the delay time. This observation can be proved rigorously. By plugging Eq. (2.26) and Eq. (2.27) into Eq. (2.26) one obtains

$$\begin{aligned} B_n &= f_\pi \cdot \int_0^\infty \left| \frac{G_{mg} \exp\left(-\pi f'/2\right)}{f' + G_{mg} \exp\left(-\pi f'/2\right)} \right|^2 df' = \beta f_\pi \\ I_p &= \frac{1}{f_\pi} \cdot \int_0^\infty \left| \frac{1}{f' + G_{mg} \exp\left(-\pi f'/2\right)} \right|^2 df' = \alpha / f_\pi \end{aligned} \tag{2.28}$$

where $f' = f / f_\pi$ is the normalized frequency, $G_{mg} = K_{dc} / \left(K_{dc}\right)_{\max}$ is the gain margin, α and β are dimentionless numbers which only depend on the gain margin. Next I plug Eq. (2.28) back into Eq. (2.27) and get

$$\sigma_{\phi_e}^2 = \alpha \frac{\Delta f}{\pi f_\pi} + \beta f_\pi \frac{e\left(P_m + P_s\right)}{R P_m P_s} \tag{2.29}$$

Using typical values for $\Delta f \sim 1MHz$ for SCLs, $G_{mg} = 8dB$, $R \sim 0.5 A/W$, $P_s \sim 1mW$, $P_m \sim 0.01mW$ and $f_\pi \le 100MHz$, I estimate that the second term ($\sim 10^{-6} rad^2$) is much smaller than the first term($\sim 0.01 rad^2$) in Eq. (2.29). Therefore $\sigma_{\phi_e}^2$ only depends on the normalized laser linewidth, i.e., $\sigma_{\phi_e}^2 = \alpha \Delta f / \pi f_\pi$. In Fig. 2. I plot the variance of the differential phase error as a function of the normalized summed laser linewidth $\Delta f / f_\pi$. If one uses T_{cs}=10years as the figure of merit for a high performance OPLL, the summed laser linewidth has to be smaller than ~1/60 of $f_\pi = 1/4\tau_d$. When fiber optical components are used, τ_d is typically 5 ns. It can be reduced to ~0.5 ns if microoptics are used instead. The corresponding summed laser linewidth has to be smaller than ~0.8MHz or ~8 MHz separately to achieve T_{cs}=10years.

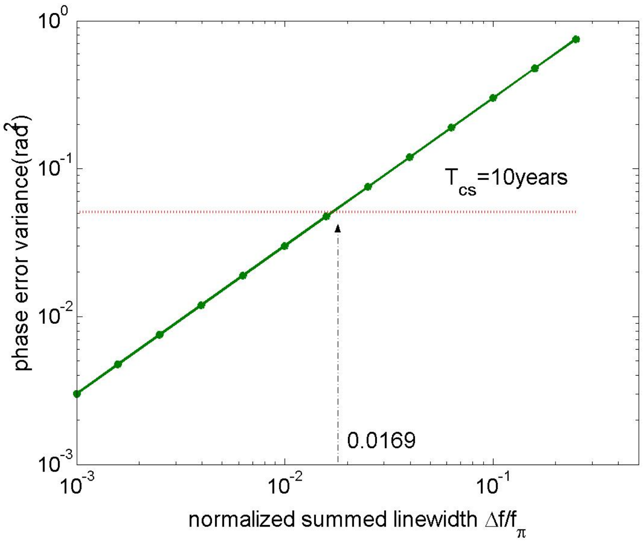

Fig. 2.7 The variance of the differential phase error as a function of the normalized summed laser linewidth $\Delta f / f_\pi$. $f_\pi = 1/4\tau_d$ is the π phase lag frequency given by the loop delay. T_{cs} is the average time between cycle slips defined in Eq. (2.25).

2.5.2 The non-uniform frequency modulation (FM) response of SCLs

In an SCL based OPLL, the SCL acts as a current-controlled oscillator (CCO) and its frequency is directly modulated by the current feedback signal[34, 35]. In the previous analysis I have assumed that the slave laser is an ideal CCO with a flat FM response. In practice, the FM response of SCLs is not uniform and exhibits different characteristics depending on the range of the modulation frequency. For a typical single-section SCL, the low frequency (smaller than 10MHz) FM response is dominated by the thermal effect and the carrier-induced effect. At the intermediate frequency (above 100MHz), the thermal effect fades out and the carrier-induced effect is the summation of an adiabatic term and a transient term[35]. As the modulation frequency further increases to a few GHz, the relaxation resonance effect becomes significant. All these phenomena contribute to the FM response and need to be examined in the OPLL analysis.

First, the relaxation resonance effect is excluded in this analysis since it is significant only at frequencies above a few GHz, which is far beyond the OPLL bandwidths (< 10MHz) encountered in this work.

In the intermediate frequency range, the FM response is composed of two terms, the adiabatic term and the transient term[35]. Using the results of [35], the current-phase modulation of a SCL is given by

$$\frac{d\phi_s}{dt} = A\frac{d}{dt}i + Bi \tag{2.30}$$

where A and B are respectively the adiabatic and the transient modulation coefficients, and i is the modulation current. Taking the Fourier transform of Eq. (2.30) and substituting it into Eq. (2.10), the open loop transfer function becomes

$$G_{op}\left(s\right) = \frac{K_{dc}}{s}\left(1 + \frac{A}{B}s\right)\exp\left(-s\tau_d\right) \tag{2.31}$$

In Eq. (2.31) A/B is typically around 10^{-11}[35], which means the adiabatic term becomes significant only at frequencies above 1 GHz. One can thus ignore its effect within the typical OPLL bandwidths studied in this work.

At frequencies smaller than 100MHz, the FM response of SCLs is composed of the thermal effect and the carrier-induced effect. While the carrier-induced effect is in phase with the modulation current and results in a blue shift with increasing current, the thermal effect is out of phase with the modulation current and produces a red shift. Due to the competition between the thermal and the carrier-induced effects, the FM response of a single section SCL exhibits a characteristic π phase reversal in the frequency range 100 kHz~10 MHz[23]. Compared to the loop delay, this phenomenon imposes a more serious constraint on the achievable loop bandwidth[22, 23, 36]. In this section I will analyze the influence of the thermal FM response on the performance of an OPLL.

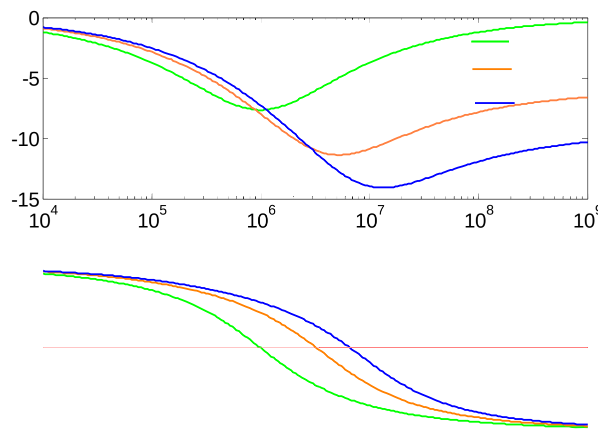

Fig. 2.8 FM response of single-section DFB lasers calculated with the modified low-pass filter model. The fitting parameters are: $f_c = 1MHz$ and b = 1, 2 and 3.

The thermal effect dominates at low frequency and fades out with the increase of the modulation frequency. Employing a modified low-pass filter model, an empirical FM transfer function of the thermal effect is given by[23, 37]

$$H_{th}(f) = -K_{th} \cdot \frac{1}{1+\sqrt{jf/f_c}} \tag{2.32}$$

where K_{th} is the thermal FM efficiency in Hz/mA and f_c is the thermal cut-off frequency. The fitting parameter f_c is structure-dependent and is typically in the range of 10kHz-10MHz[22]. The carrier-induced FM response is flat from DC to frequencies in the neighborhood of the relaxation frequency, and is in phase with the modulation current, i.e.

$$H_{el} = K_{el} \tag{2.33}$$

Combining the thermal and carrier-induced effects, the total FM response is described by

$$H_{FM}^{DFB}(f) = -\frac{K_0}{b}\left(\frac{b-\sqrt{jf/f_c}}{1+\sqrt{jf/f_c}}\right) \tag{2.34}$$

where K_0 is the DC current-frequency tuning sensitivity and $b = K_{th}/K_{el} - 1$ is related to the relative strengths of the carrier-induced effect and the thermal effect. In Fig. 2.8 I plot the FM responses for $f_c = 1MHz$ and b = 1, 2 and 3, respectively.

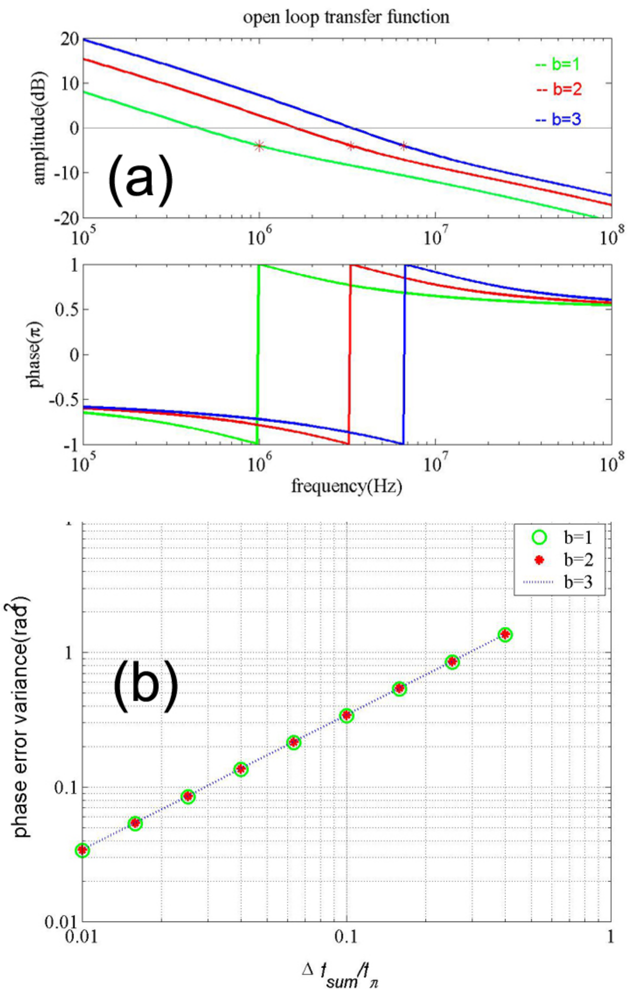

Fig. 2.9 (a) The Bode plots of the open loop transfer functions for different values of the fitting parameter b in Eq. (2.34). (b) The variance of the differential phase error as a function of the normalized laser linewidth $\Delta f / f_\pi$.

Substituting Eq. (2.34) into Eq. (2.10), I proceed to calculate the open loop transfer function and the results are plotted in Fig. 2.9(a). The gain margin is 8 dB and the other parameters are the same as those in Fig. 2.8. The corresponding π phase lag frequencies f_π are 1, 3.2 and 6.6MHz respectively. I further calculate the variance of the differential phase error with Eq. (2.22). The results are shown in Fig. 2.9(b) as a function of the normalized summed laser linewidth $\Delta f / f_\pi$. Similar to the loop delay case, the variance of the differential phase error only depends on $\Delta f / f_\pi$ for a given gain margin.

In conclusion, to phase lock SCLs with reasonably small residual differential phase error, the summed linewidth has to be significantly smaller than the loop bandwidth. The bandwidth of the OPLL, however, is limited to a few MHz due to the non-uniform FM response of the single section SCLs. Historically, specially designed SCLs, such as multi-section DFBs, have been demonstrated to have flat FM response up to a few GHz[11]. However, these lasers are not commercially available and their stability needs to be improved. On the other hand, the linewidth of SCLs can be reduced by introducing optical feedback. Therefore external cavity SCLs with sub-MHz linewidth have been used to build OPLLs. In the next chapter, I will present and characterize the experimental study of OPLLs built using different commercial SCLs.